On liver modelling under trauma situations

Cécile Conte, Catherine Masson, Nicolas Cheynel, Pierre-Jean Arnoux

Journal of Biological Physics and Chemistry 9 (2009) 167–170

On liver modelling under trauma situations

C. CONTE*†, C. MASSON†, N. Cheynel† and P.J. ARNOUX†

† Laboratoire de Biomécanique Appliquée, INRETS/Université de la Méditerranée, Bd P. Dramard 13916 MARSEILLE Cedex 20, FRANCE

*Corresponding author Email: cecile.conte@inrets.fr

Abstract

Thoracic and abdominal organs are highly injured during crash situations leading to severe traumas with high morbidity. To prevent this, the definition of efficient safety devices should be based on a detailed knowledge of injury mechanisms and related injury criteria. In this sense, FE simulation coupled to experiment could be a valuable tool to provide a better understanding of internal organs behaviour. This preliminary study aims to improve FE model focussing on liver mechanical behaviour. It concerns the identification of structure mechanical properties up to the evaluation of damage occurrence. This work intends to build a methodology to implement the liver behaviour in a FEM that is robust enough to describe the biological, intrinsic and experimental variability. It is based on an ongoing experimental characterisation of the liver under quasi-static compression. A first set of model parameters, relevant with the sub injury level was first obtained. Then, the damage evaluation was performed through Von Mises levels analysis by comparison to the experimental tests including necropsies and histological structure analysis. Results highlights that damage was centred in the middle part of the right lobe. This let us complete understanding on injury mechanisms and clinical data of liver traumas.

Keywords: abdominal organs, FE simulation, inverse analysis, damage evaluation

Short title: On liver modelling under trauma situations

1. Introduction

Thoracic and abdominal organs are usually simulated in finite elements models (FEM) of the human body using viscoelastic or hyperelastic behaviour laws [1, 2]. Experimental investigations of organs mechanical behaviour under compressive loadings follow two ways: the use of tissue samples to give a local information that must be analyzed considering border effects [3] or the whole structure behaviour evaluation [4]. This last

method, at the organ level, must be coupled to an inverse analysis to improve identification process. This work aims to build a methodology to implement the liver behaviour in a FEM that is robust enough to describe the biological, intrinsic and experimental variability. It is based on an ongoing experimental characterisation of the liver under quasi-static compression and is a preliminary to the building of a model able to describe the damage of hepatic tissues.

2. Methods

2.1. Setting of behavior law

The FEM was build from CT-scan data [5]. The Glisson's capsule, modelled using shell elements, is assumed as elastic. The parenchyme, meshed with tetra elements of characteristic length about 6 mm, was set hyperelastic with a Mooney-Rivlin law (Eq. 1 et 2). Both structures were assumed as homogeneous and isotropic.

$$W = C_{10}(I_1 - 3) + C_{01}(I_2 - 3) \qquad \text{Eq. 1}$$

$$\text{with} \quad \begin{cases} I_1 = tr(\underline{\underline{C}}) \\ I_2 = \dfrac{I_1^2 - tr(\underline{\underline{C}}^2)}{2} \end{cases} \qquad \text{Eq. 2}$$

where W is the Helmholtz free energy function, I_1 et I_2 are the two first invariants of the Cauchy tensor $\underline{\underline{C}}$ and C_{10} et C_{01} are two parameters of the law expressed in MPa.

2.2. Inverse analysis method

Model parameters were quantified through experimental uniaxial compression tests in the rear to front direction at 0.001 m/s (Figure 1). The experimental corridor (black curves in

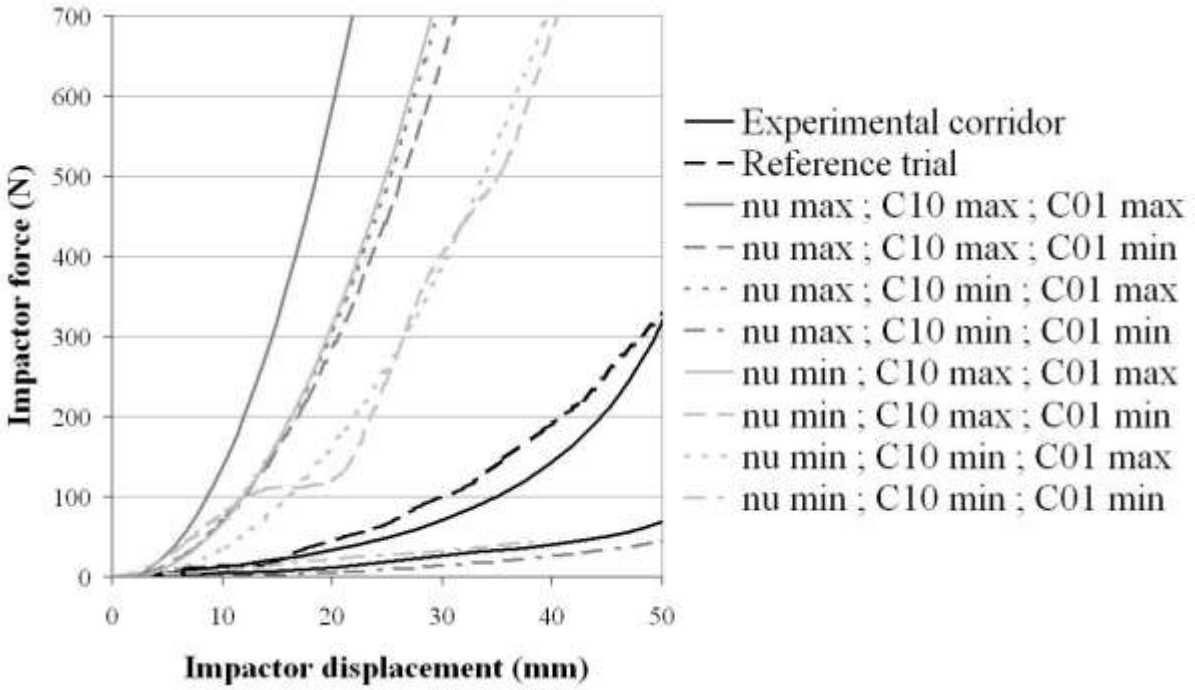

Figure 2) was build from the first results of this campaign. The identification methodology was based on an inverse analysis methodology which followed three steps:

Step 1: Space of potential responses exploration. In order to define the set of parameters for the behaviour law the design of experiments methods was used. The sampling method chosen was a 2 levels complete factorial design [6] with 4 factors (parenchyma density d and Poisson's coefficient ν, C_{10} and C_{01}) (Table 1). The response of a given treatment was the evaluation function Y definied by Eq. 3. Y was the average of relative difference between the force needed to reach a displacement u_i in the treatment configuration $F_{treat}(u_i)$ and in a reference one $F_{ref}(u_i)$:

$$Y = \frac{1}{N}\sum_{i=1}^{N}\frac{\left|F_{treat}(u_i) - F_{ref}(u_i)\right|}{F_{ref}(u_i)} \qquad \text{Eq. 3}$$

N is the number of points of the response curve. The reference configuration (grey curve in Figure 2) is: d = 0.001 g/mm^3, ν = 0,495, C_{10} = 0.003 MPa and C_{01} = 0.011 MPa.

Step 2: Model optimisation using a NLPQL method [7] applied to the relevant set of parameters of step 1. The optimisation function definition was the same as for the evaluation function replacing the reference curve in Eq. 3 with a standard curve of the upper part of the corridor obtained during a second experimental campaign. To attenuate geometrical differences between experimental and numerical livers, relative displacements defined by $u_{i\,rel} = \frac{u_i}{th_0}$ (th_0 being the liver initial thickness) are used instead of effective displacements u_i.

Step 3: Robustness analysis of the optimised model. Effects of isolated and crossed variations of the influent parameters were investigated in the neighbourhood of their optimal value (±10%).

2.3. Damage observation

As a first step toward damage integration in the model, the areas of potential damage are computed using the optimised model and compared to those noticed during the experimental tests. At the moment, the maximal values of the Von Mises equivalent stress were used as a way to isolated stress concentration areas which could be associated to damage occurrence in first approximation.

3. Results

3.1. Inverse analysis

The mean evaluation function obtained for the 16 treatments of the step 1 was 462%. The model sensitivity to one parameter *p* was evaluated calculating the corresponding contrast:

$$c(p) = \sum_{i=1}^{N_{treat}} l_i Y_i \qquad \text{Eq. 4}$$

where N_{treat} is the number of treatments performed for the design, Y_i is the computed evaluation function and l_i is the level of *p* for the treatment *i* (-1 if *p* is minimum and +1 if *p* is maximum)

p was considered as influent once its contrast reached 5 (Table 1). The model was then independent of the density (alone or interacting with another parameter). On the other hand, with the used behaviour law the model exhibited a high sensitivity to *v*, C_{10} and C_{01} with a high dispersion of the responses (Table 1 and

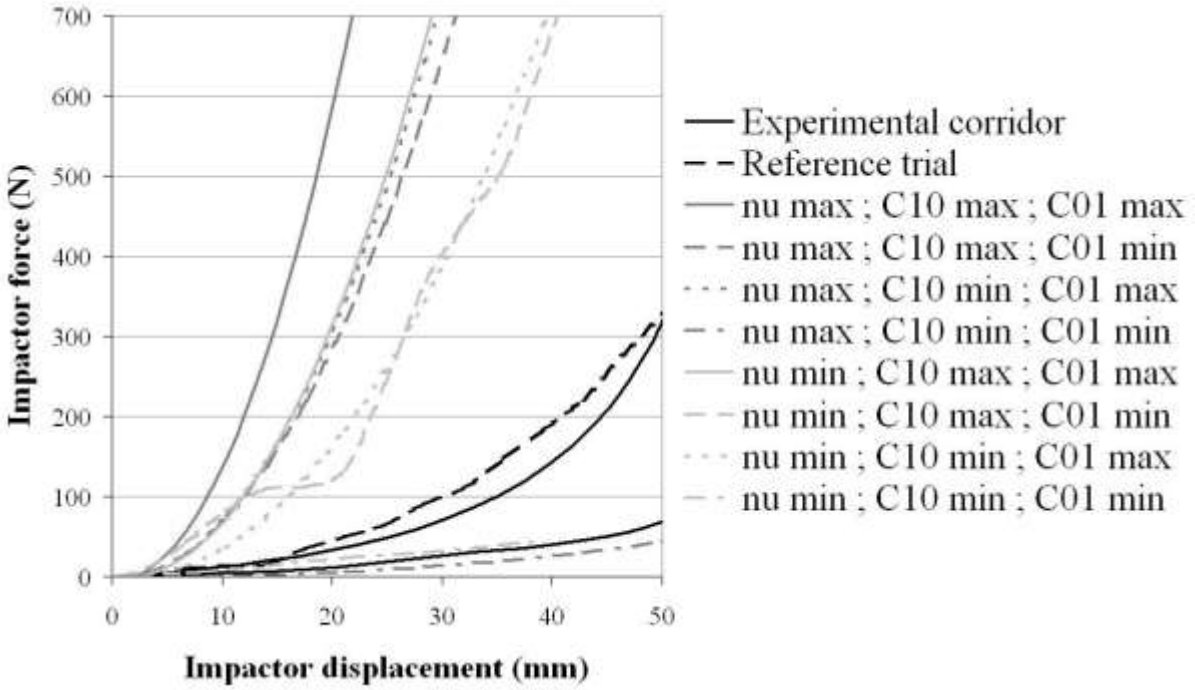

Figure 2). The initial slope of curves increased with the modules and decreased with v. Lastly, as C_{10} and C_{01} had a similar effect, their variation ranges were assumed as the same. Three configurations were then selected, giving the following variation ranges: C_{10} and C_{01} between 0.001 and 0.005 MPa and v between 0.2 and 0.495.

Optimisation (step 2) is performed within these variation ranges on the three influent parameters. The final set of parameters was chosen on the bases of the optimisation process ($Y \leq 0.2$) and relevance with corridors data. After 25 runs of the NLPQL algorithm, the optimised set of parameters is: v = 0.4, C_{10} = 0.005 MPa and C_{01} = 0.003 MPa. For this set of parameters, the optimisation function scored 0.18, which represents a suitable deviation between experiment and simulation in the elastic phase of the compression process where damage does not occur yet (

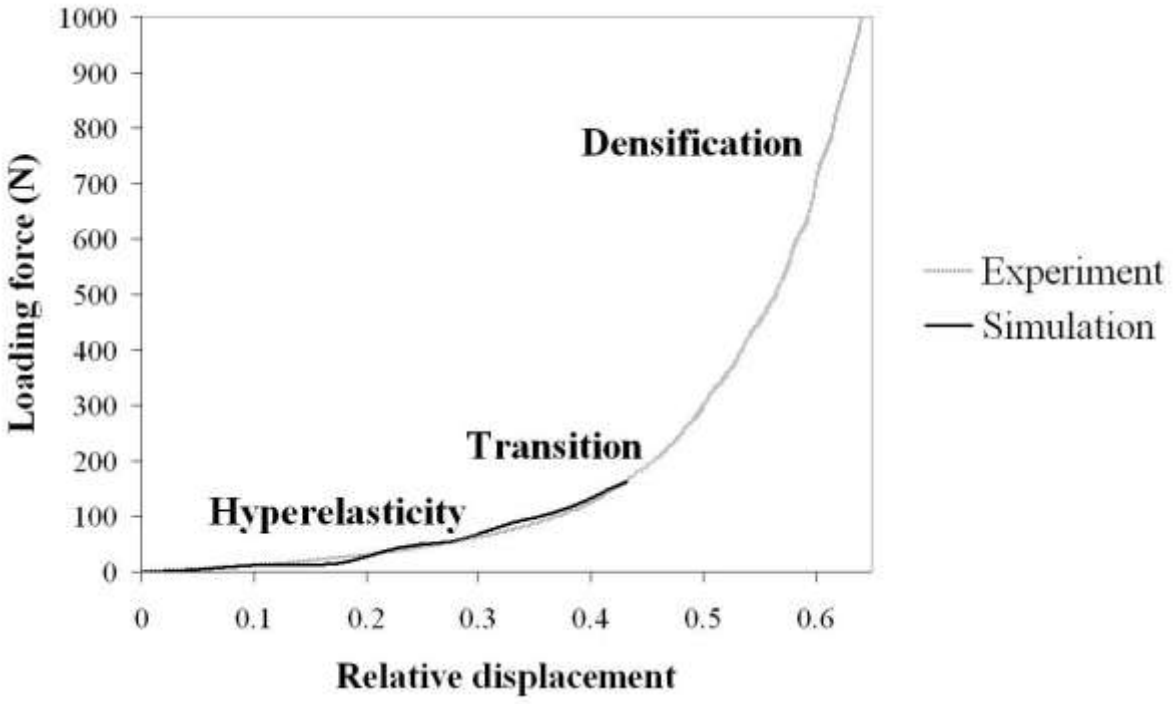

Figure 3). Moreover, the value of ν is consistent with the hypothesis of incompressibility currently assumed [8].

3.2. Damage observation

An approximate three-dimensional distribution of failure observed with experiments is given in the

Figure 4. We can then isolate 5 cracks: 3 are independent and 2 are coupled and form the main crack. Their direction of propagation is the right-left axis of the liver (x-axis in Figure 1) and the crack plan is vertical (xz-plan in Figure 1). This result is consistent with the common assumption that forces controlling the failure are normal to the loading direction and oriented from the centre to the surface of liver because of the organ spreading.

On simulation, the maximal Von Mises equivalent stress reached is 0.040 MPa. As a comparison, the critical stress in traction for liver is between 0.066 and 0.386 MPa [9] which confirms that the model reaches an acceptable stress order at the end of the elastic phase of the compression. At this level, the areas of potential damage (three higher levels of Von Mises stress) are roughly relevant with the experimental cracks (

Figure 5) in term of location and direction. Failure is located only in the right lobe and is maximal near the hilum. However, in the simulation, the area is larger in the vertical direction (along the z-axis in Figure 1) and less extensive in the lateral one (along the x-axis in Figure 1). Notes the secondary cracks are not present with simulations. These results show that in first approximation the current model can be adapted to describe damage and failure of the liver.

4. Discussion and conclusion

This work describes an integrated approach coupling exploration, optimisation and robustness analysis. Applied to the liver, this approach was used to isolate the admissible set of influent parameters including their potential variations to fit a hyperelastic law. A first set of parameters was defined to simulate in this FE model the liver behaviour up to the damage phase. For the material behaviour, accuracy could also be improved by adding viscous component to describe strain rate effects [2].

The comparison between experimental damage location and model simulation was performed using stress distribution in the structure. The results obtained showed the same structure effects with high stress concentration on the middle part of the organ and confirmed assumption of opening and spreading failure modes within the liver structure. Damage evaluation could be improved determining a dedicated criterion. This point should be related to coupling of a damage model in addition to the initial behaviour law. Simulation results will best fit experimental observation by having a method to physically implement failure process in the model. At this stage and regarding meshing choices performed, a kill element method could be used. By the way, a more accurate modelling of the structure is necessary to improve description of the crack initiation and propagation. In particular, the main vascular structures which concentrate stresses and the global geometry which is different from one liver to another must be taken into account.

A strong variability was observed on experimental data. So in a further step, the objective will be to determine relationship between the variation ranges of parameters and the potential biological variability of the experimental population. At least, this methodology can be extended to more complex model such as hyper-viscoelastic model including damage and failure.

5. Bibliography

1. Carter, F.J., Frank, T.G., Davies, P.J., McLean, D., and Cuschieri, A. Measurements and modelling of the compliance of human and porcine organs. *Medical Image Analysis*. **5** (2001) 231-236.
2. Miller, K. Constitutive modelling of abdominal organs. *Journal of Biomechanics*. **33** (2000) 367-373.

3. Chui, C., Kobayashi, E., Chen, X., Hisada, T., and Sakuma, I. Transversely isotropic properties of porcine liver tissue: experiments and constitutive modelling. *Med Bio Eng Comput*. **45** (2007) 99-106.
4. Farshad, M., Barbezat, M., Flüeler, P., Schmidlin, F., Graber, P., and Niederer, P. Material characterization of the pig kidney in relation with the biomechanical analysis of renal trauma. *Journal of Biomechanics*. **32** (1999) 417-425.
5. Labé, A. Etude des mécanismes lésionnels de la région abdomino-pelvienne. Applications à la traumatologie virtuelle et à la sécurité routière. *Université de la Méditerranée Aix-Marseille II* (2008).
6. Clément, B. Plannification et analyse statistique d'expérience. *Document de cours, Ecole Polytechnique de Montréal, Département de mathématiques et de génie industriel*. (2006).
7. Schittkowski, K. NLPQL: A Fortran subroutine for solving constrained nonlinear programming problems. *Annals of Operations Research*. **5** (1985/86) 485-500.
8. Saraf, H., Ramesh, K.T., Lennon, A.M., Merkle, A.C., and Roberts, J.C. Mechanical properties of soft human tissues under dynamic loading. *Journal of Biomechanics*. **40** (2007) 1960-1967.
9. Stingl, J., Baca, V., Cech, P., Kovanda, J., Kovandova, H., Mandys, V., Rejmontova, J., and Sosna, B. Morphology and some biomechanical properties of human liver and spleen. *Surg Radiol Anat*. **24** (2002) 285-9.

Tables:

			Direct influences	Coupled influences	
Factors	Min.	Max.	Direct contrast	Second factor	Interaction contrast
Density d in g/mm^3	0.0005	0.0015	3	v	4
				C_{10}	2
				C_{01}	1
Poisson coefficient v	0.2	0.495	25	C_{10}	13
				C_{01}	13
Module C_{10} in MPa	0.001	0.1	31	C_{01}	5
Module C_{01} in MPa	0.001	0.1	35		

Table 1. Values and influences of the design factors: for each factor, minimal and maximal values are used for the exploration of responses space. Their influence, alone or in interaction with another factor, is computed using Eq. 4.

Captions of figures:

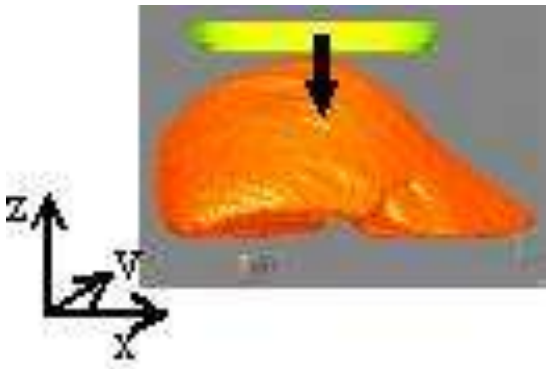

Figure 1. Rear to front compression of the liver.

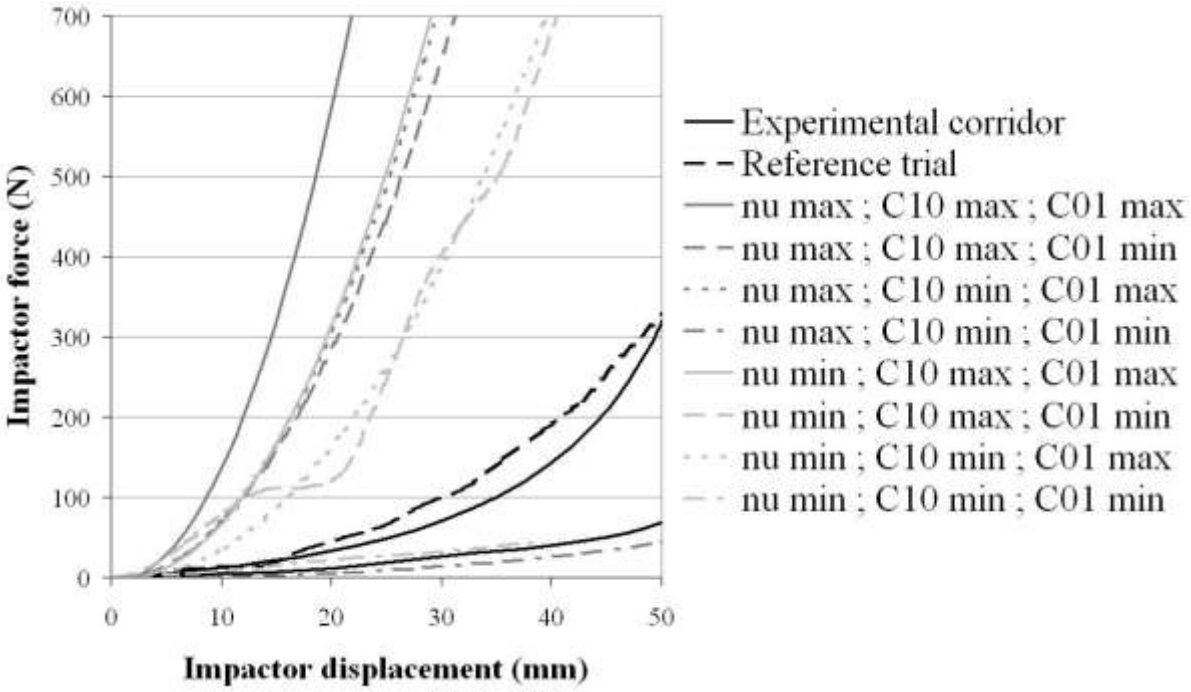

Figure 2. Responses of the influent treatments.

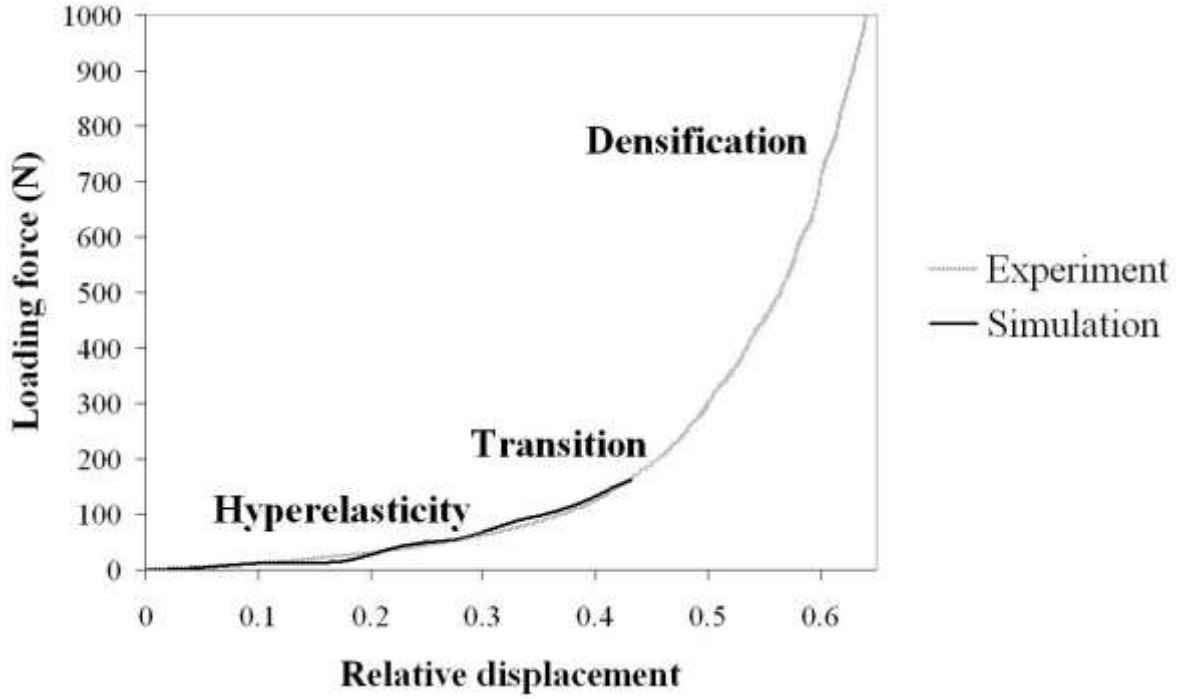

Figure 3. Response of the optimised model in the elastic phase of the compression.

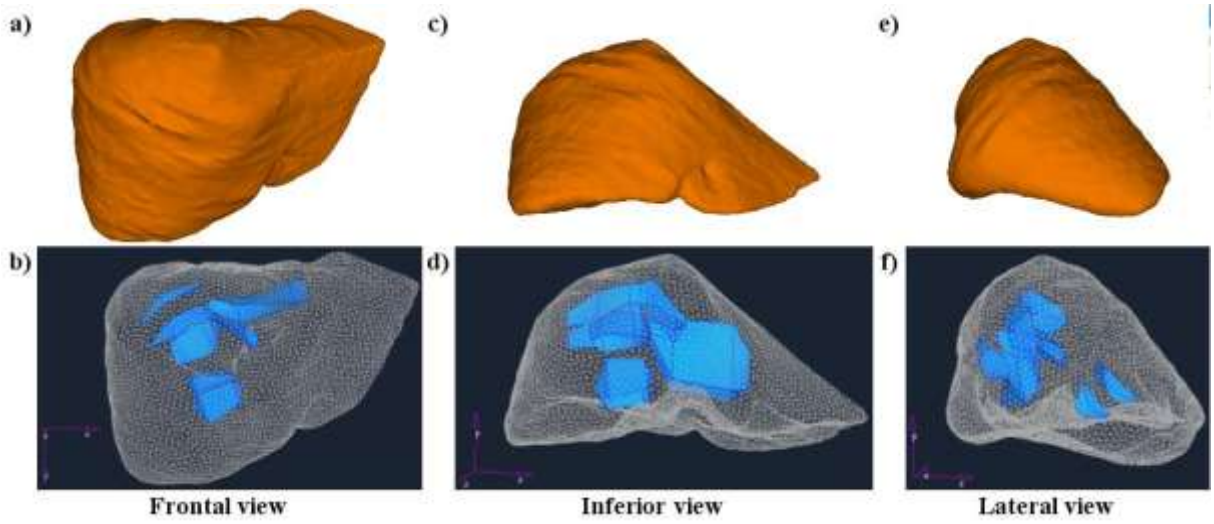

Figure 4. 3D localisation of experimental damage: a, c and e are visualisations of the external surface whereas b, d and f are internal visualisations of the liver in frontal, inferior and lateral view (respectively). The blue 3D-components stand for the surface of failure observed experimentally.

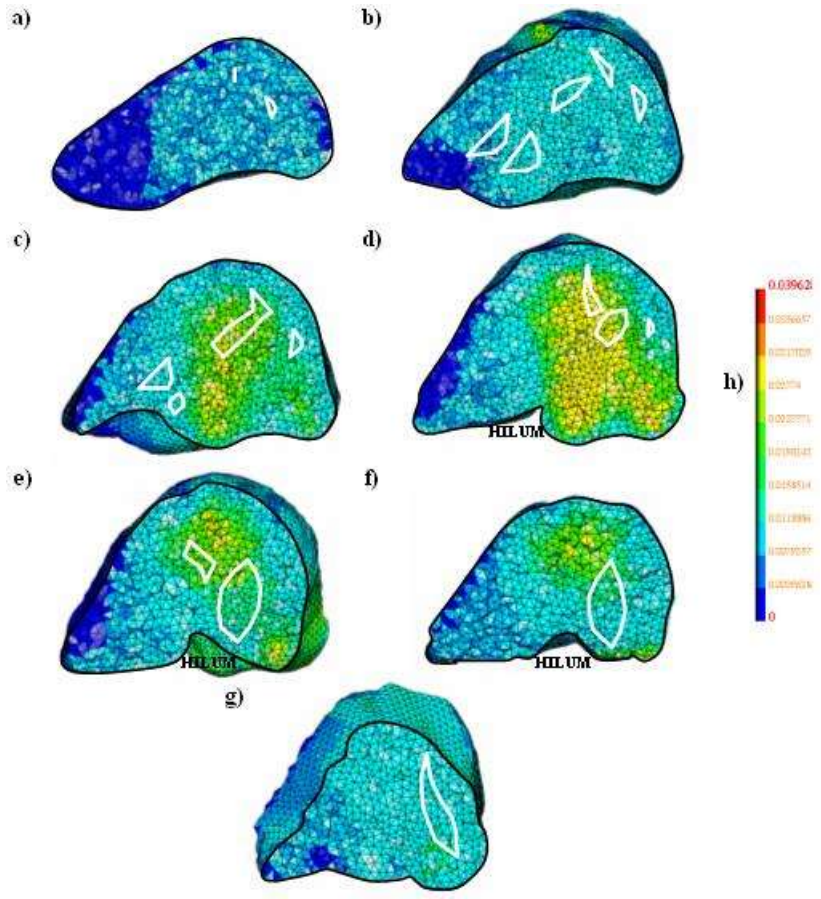

Figure 5. Comparison between maximal Von Mises equivalent stresses localistion after simulation and experimental failure areas: a, b, c, d, e, f and g show sections of the right lobe of the liver model by sagittal plans from right to left. Contours of the section are lined in black, those of experimental cracks are lined in white. h gives the Von Mises equivalent stress levels in MPa.